Northeastern University

Robot Sensing and Navigation - EECE5554
LAB 5 Analysis Report

VARUN SAMALA

Introduction

we will explore the application and importance of using calibrated cameras to create basic photomosaics. For the purposes of this lab, a smartphone camera was utilized to capture all the necessary images. A set of 15 images featuring a checkerboard pattern were specifically employed for the camera calibration exercise.

Camera calibration

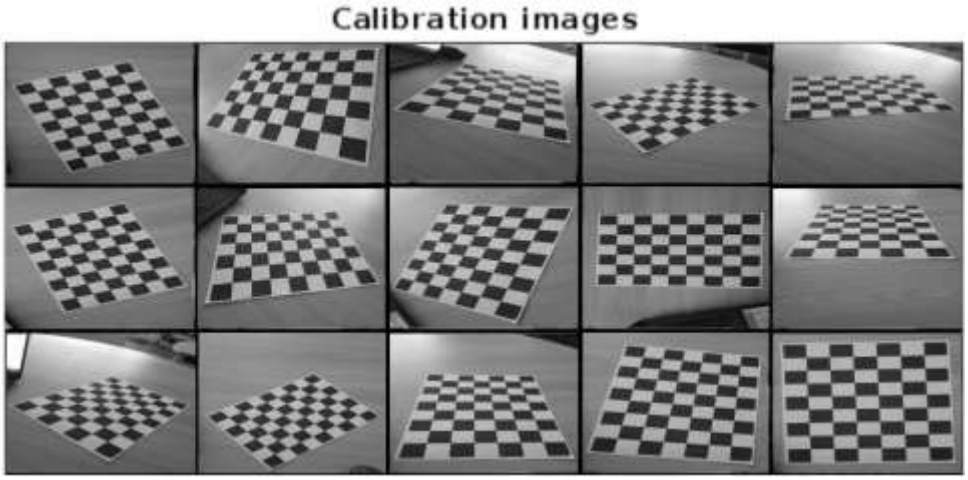

Fig. 1 Camera images of checkerboard used for calibration.

For calibrating the camera, the Caltech camera calibration toolbox was applied to the checkerboard images. These images underwent a process where corners were automatically detected to count the squares on the grid. Each square in the grid measured 30mm along both the x and y axes, with the grid consisting of 7 squares along the x-axis and 5 along the y-axis. This corner detection process was repeated for all the images. After calibration, the reprojection error was calculated and documented as illustrated.

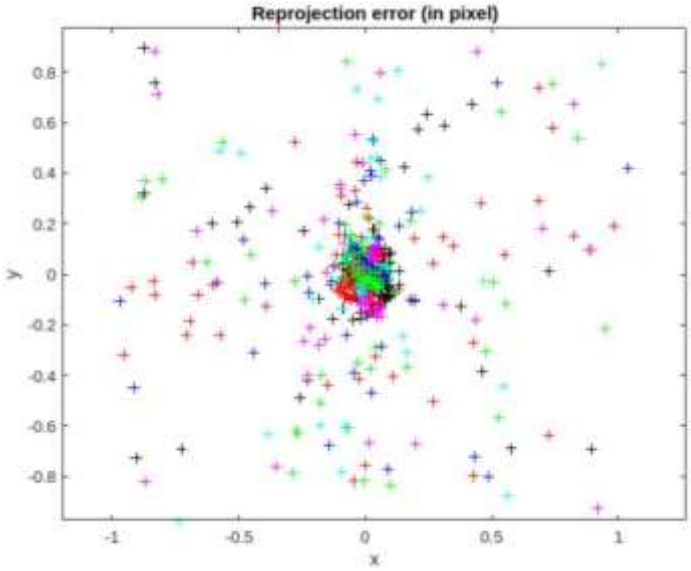

Fig. 2 Reprojection Error in pixel.

The calibration parameters, along with the error values, were determined following an automated re-evaluation of the corners and the exclusion of images with significant errors. The results are detailed as follows:

Error = [0.24269, 0.24310]

```
Main calibration optimization procedure - Number of images: 15
Gradient descent iterations: 1...2...3...4...5...6...7...8...9...10...11...12...13...14...15...16...done
Estimation of uncertainties...done


Calibration results after optimization (with uncertainties):

Focal Length:          fc = [ 3614.07509   3615.40624 ] +/- [ 3.21111   3.12029 ]
Principal point:       cc = [ 1575.42211   1055.83646 ] +/- [ 2.44584   3.58891 ]
Skew:             alpha_c = [ 0.00000 ] +/- [ 0.00000  ]   => angle of pixel axes = 90.00000 +/- 0.00000 degrees
Distortion:            kc = [ -0.09205   0.09898   -0.01467   -0.00298  0.00000 ] +/- [ 0.00126   0.00254   0.00021   0.00014  0.00000 ]
Pixel error:          err = [ 0.24269   0.24310 ]

Note: The numerical errors are approximately three times the standard deviations (for reference).
```

Fig. 3 Calibration parameters.

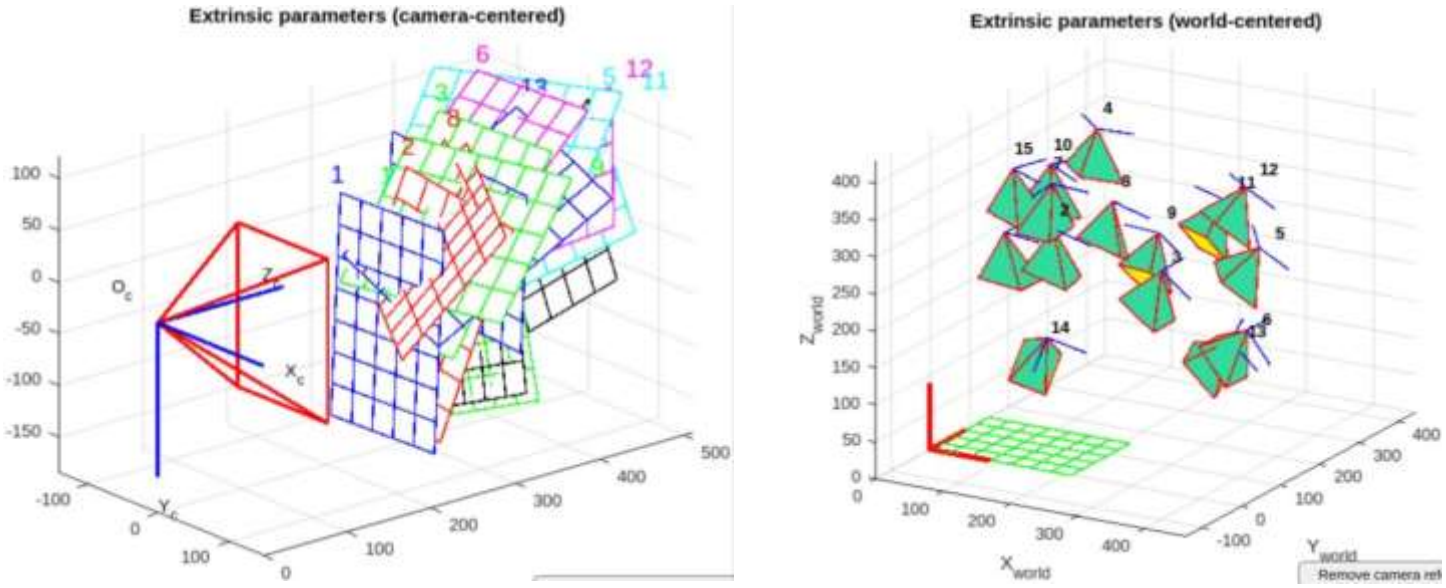

Fig. 4 Extrinsic parameters in camera-centered and world-centered view.

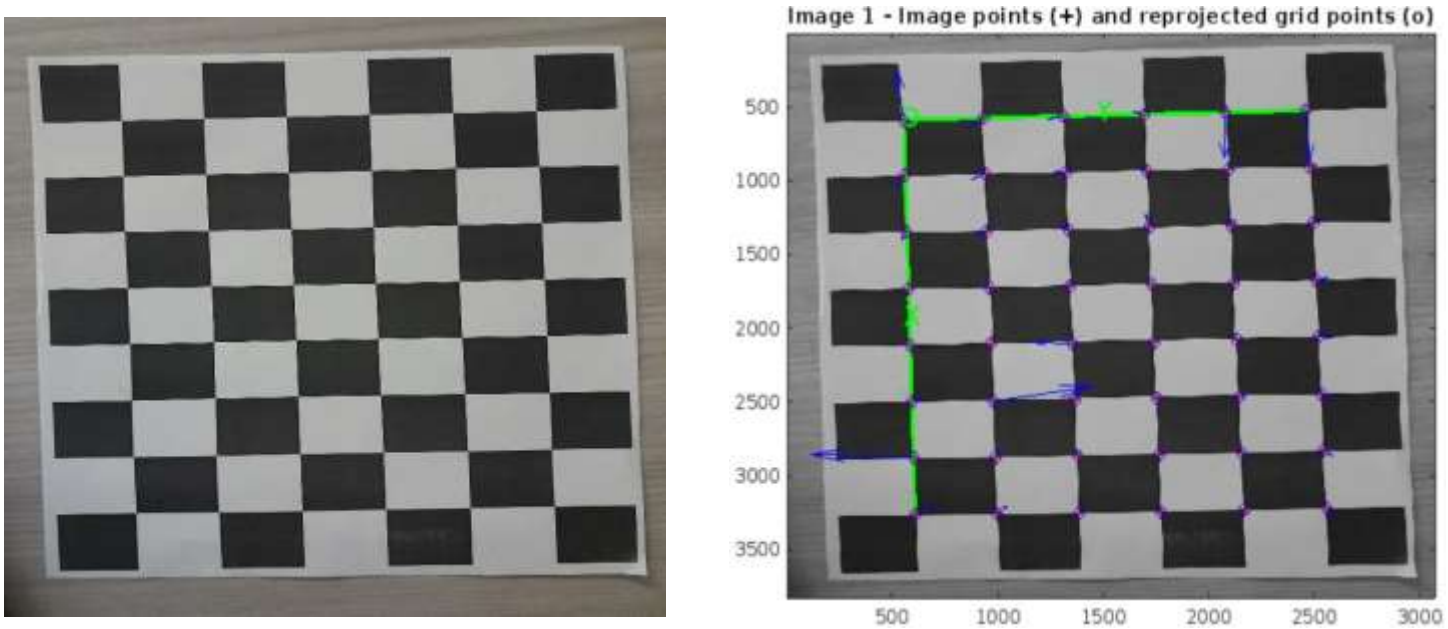

Fig. 5 Image before and after calibration. The red crosses are the grid corners.

LSC Mosaic

Photographs of the mural on the Latino Student Center building, Forsyth Street was captured as specified. Below is the image set.

Fig. 6 Latino Student Center (LSC) image set.

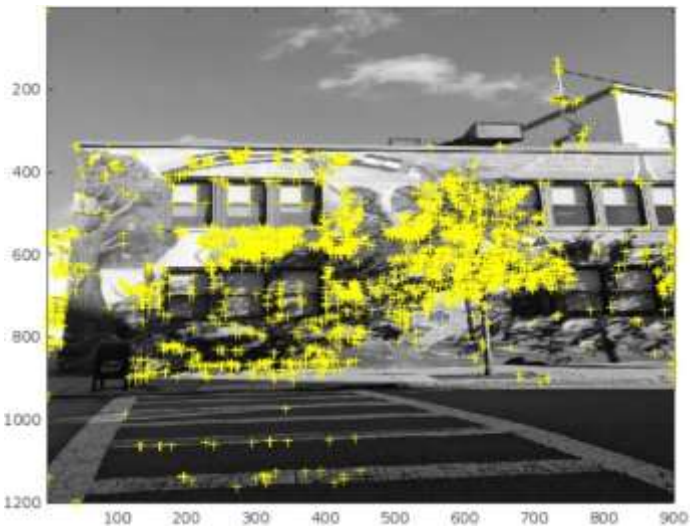

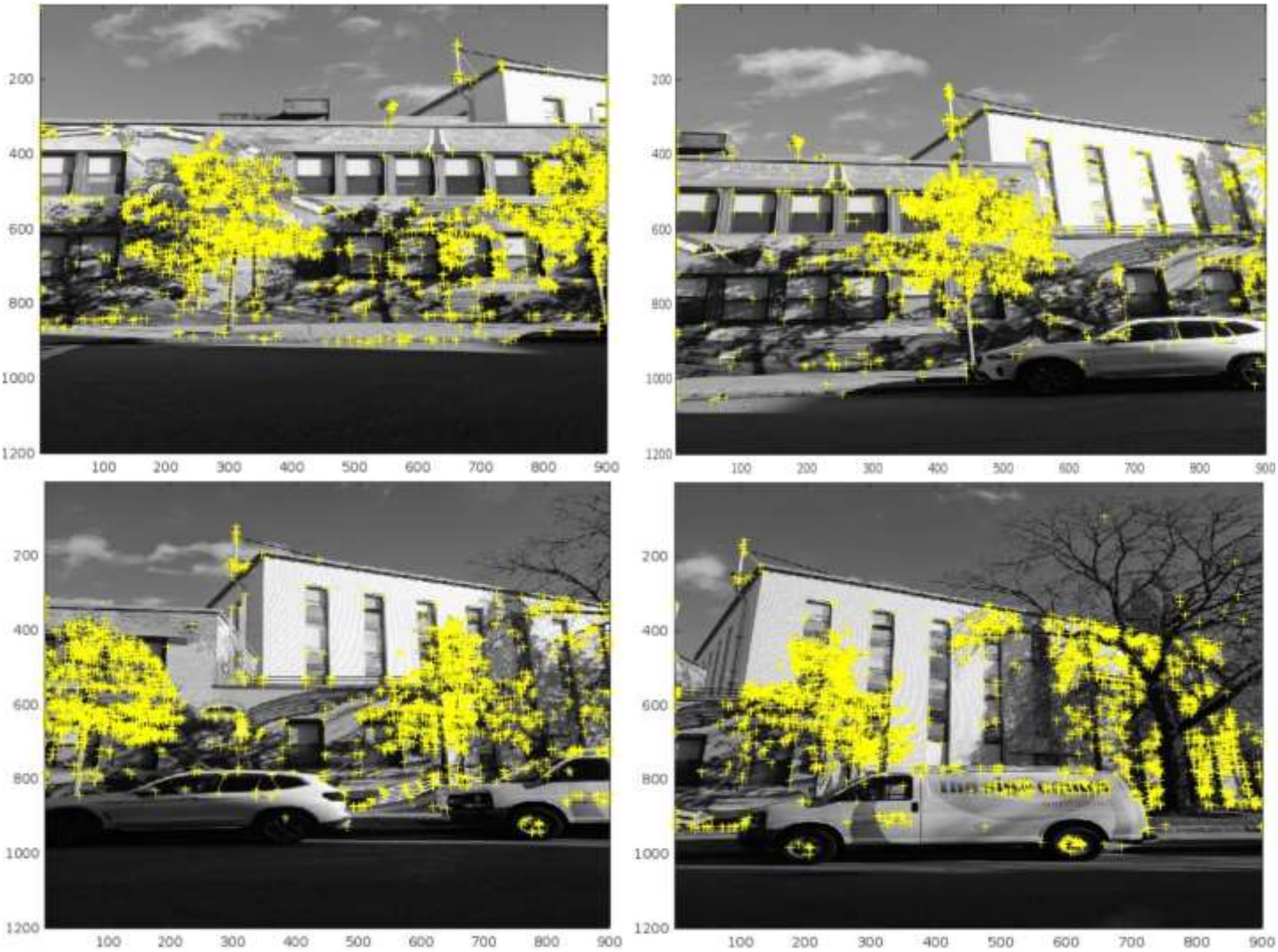

Fig. 7 Distribution of Harris corners across image set.

Fig. 8 Final LSC Panoramic Mosaic.

The Harris feature detector was employed to extract features from the LSC mural image set. Figure 7 illustrates these features, marked by yellow plus symbols, which denote the detected edges and corners of various elements like buildings, windows, trees, and cars. The process was set to identify a maximum of 2500 interest points between the images, utilizing a tile size of [2 2]. Initially, a projective transformation approach was used, which was subsequently switched to an affine transformation, maintaining a constant confidence level of 99. Affine transformations are more effective for images captured from a distance, leading to a more refined panoramic mosaic.

Brick Wall Mosaic

Fig. 9 Brick wall image set.

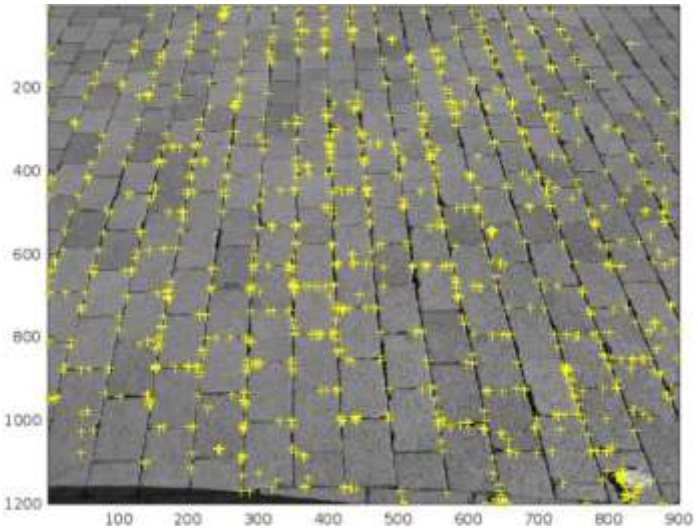

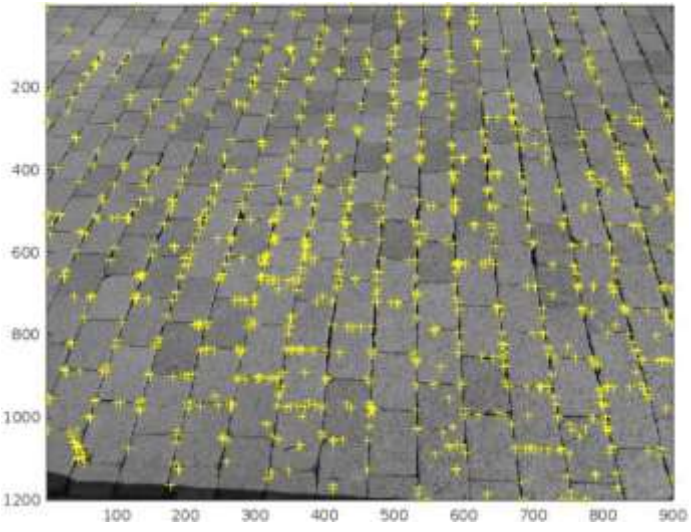

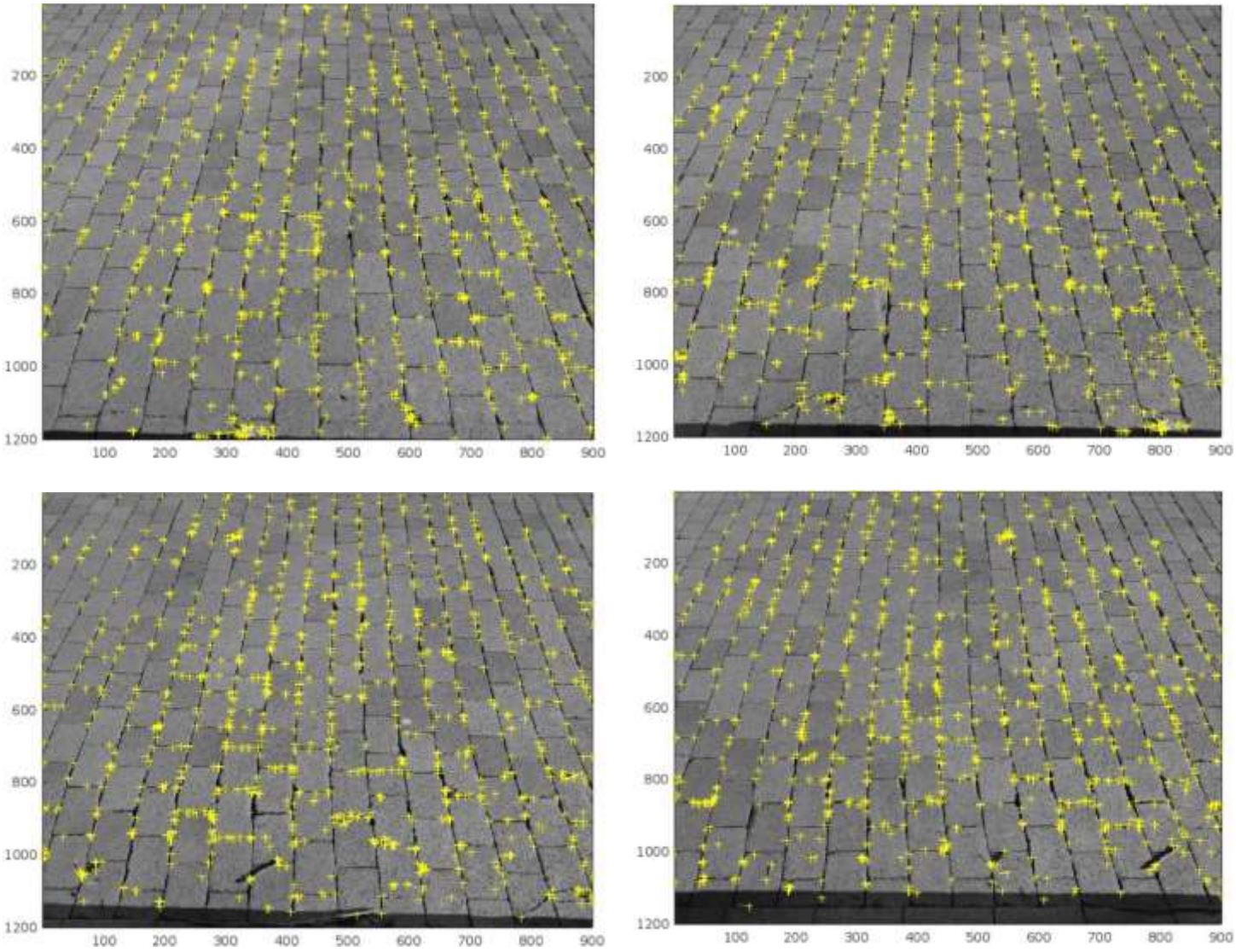

Fig. 10 Initial images with Harris corners.

Fig. 11 Final brick wall/cinder block image.

Despite using the same image capture method with a 50% overlap criterion for both the LSC and brick wall images, the brick wall mosaic exhibited superior performance compared to the LSC mosaic. In contrast to the LSC murals, the brick wall images were seamlessly stitched together using just 1000 interest points and a [2 2] tile size. As depicted in Figure 10, the Harris features were uniformly distributed across all brick wall images. This enhanced performance is attributed to the inherent characteristics of the brick pattern, which is abundant in corners and edges. In comparison, the LSC murals contain extensive 'flat' regions, such as the sky, where feature information is minimal. This difference in texture and detail facilitated more effective alignment of the brick images by the algorithm.

Third 'mosaic'

Fig. 12 Image set of graffiti with 15% overlap.

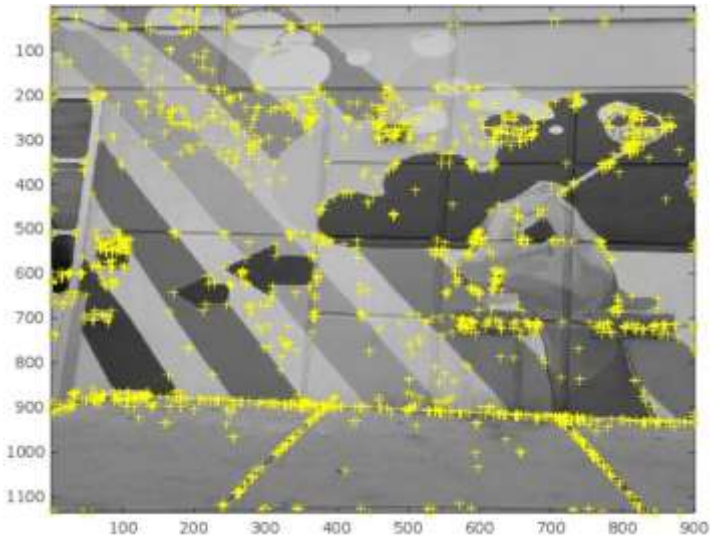

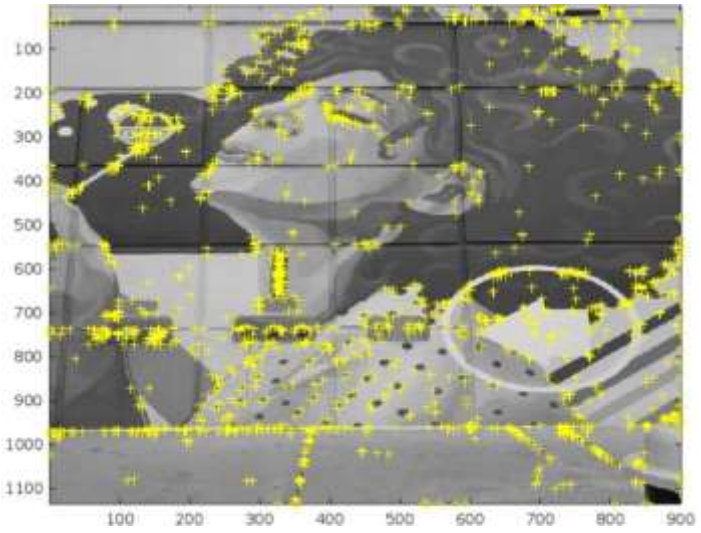

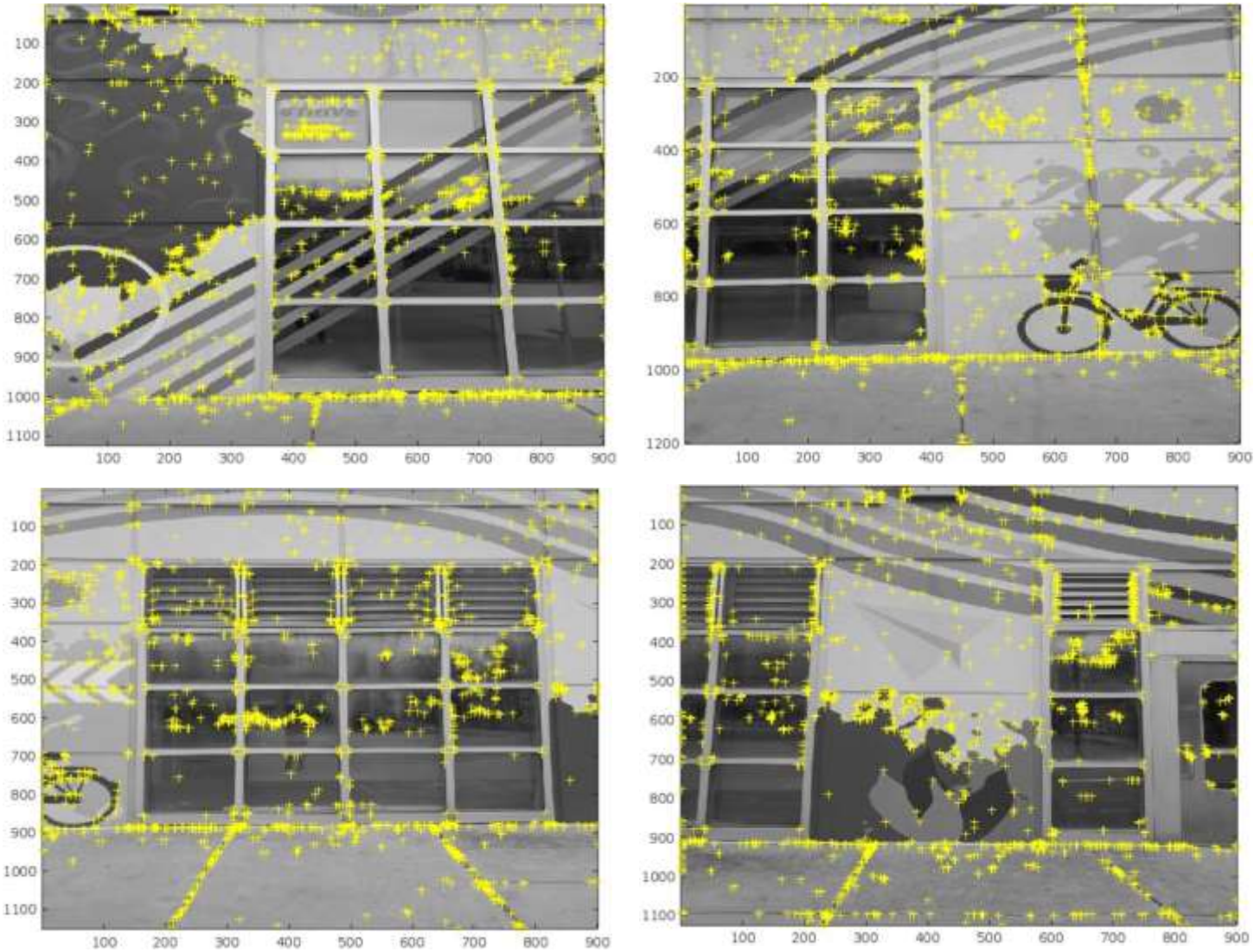

Fig. 13 Initial images with Harris corner with 15% overlap.

Fig. 14 Final mosaic with 15% overlap.

Fig. 15 Image set of graffiti with 50% overlap.

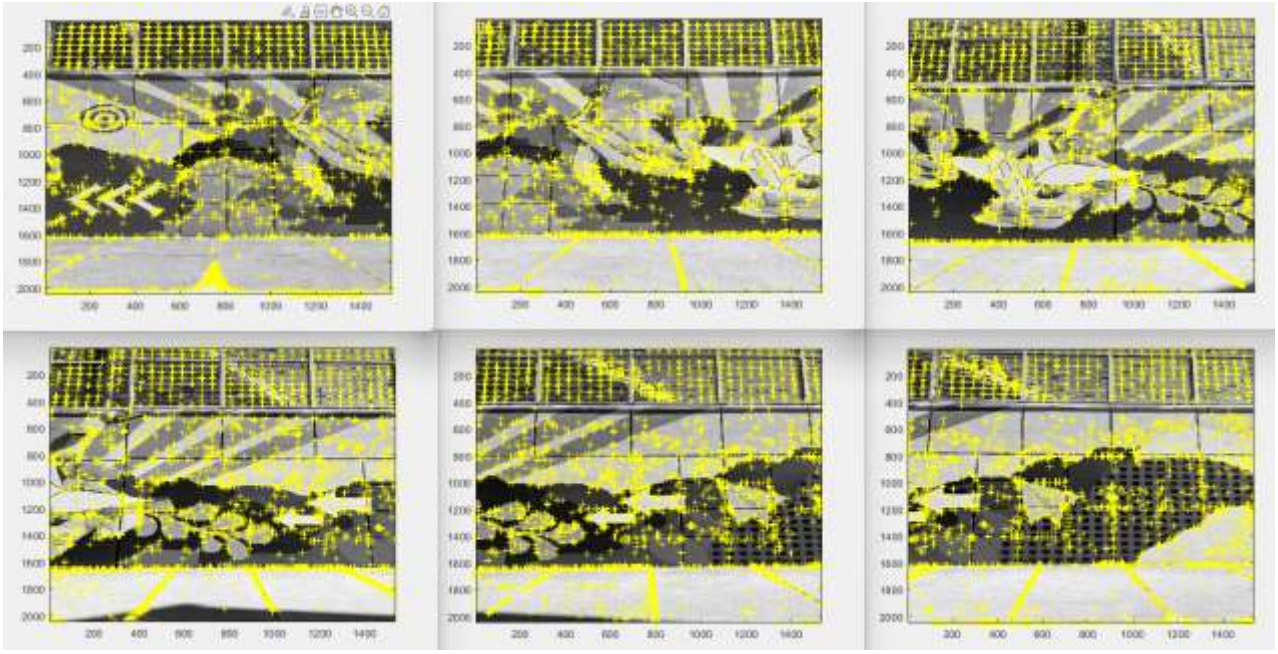

Fig. 16 Initial images with Harris corner with 50% overlap.

Fig. 17 Final mosaic with 50% overlap.

Graffiti images were captured at Ruggles station's boundary wall, with two sets having different overlap percentages: one with 15% overlap and the other with 50%. The 15% overlap in the first set of graffiti images resulted in fewer matched feature points between images compared to the 50% overlap in the second set, leading to more effective stitching in the latter. Initially, basic parameters were applied to both graffiti sets, but the first set showed poor performance due to limited feature detection by the Harris detector. To improve this, the N value, initially set at 500, was progressively increased to 1000 and then to 1500, enhancing the matching of points between images.

Another challenge involved the positioning of pixels in some images, which were significantly distant from their counterparts in preceding images, causing mismatches. This issue was addressed by adjusting the tile size incrementally from [1 1] to [2 2] and eventually to [3 3], ensuring a more uniform distribution of feature points. Conversely, the 50% overlap graffiti required only a tile size of [2 2] for successful image stitching.